

The Coulomb interaction in Helium-3:

Interplay of strong short-range and weak long-range potentials

J. Kirscher* and D. Gazit†

Racah Institute of Physics, The Hebrew University, Jerusalem 91904, Israel

Abstract

Quantum chromodynamics and the electroweak theory at low energies are prominent instances of the combination of a short-range and a long-range interaction. For the description of light nuclei, the large nucleon-nucleon scattering lengths produced by the strong interaction, and the reduction of the weak interaction to the Coulomb potential, play a crucial role. Helium-3 is the first bound nucleus comprised of more than one proton in which this combination of forces can be studied.

We demonstrate a proper renormalization of Helium-3 using the pionless effective field theory as the formal representation of the nuclear regime as strongly interacting fermions. The theory is found consistent at leading and next-to-leading order without isospin-symmetry-breaking 3-nucleon interactions and a *non-perturbative* treatment of the Coulomb interaction. The conclusion highlights the significance of the regularization method since a comparison to previous work is contradictory if the difference in those methods is not considered.

With a *perturbative* Coulomb interaction, as suggested by dimensional analysis, we find the Helium-3 system properly renormalized, too.

For both treatments, renormalization-scheme independence of the effective field theory is demonstrated by regulating the potential and a variation of the associated cutoff.

* j.kirscher@mail.huji.ac.il

† doron.gazit@phys.huji.ac.il

I. INTRODUCTION

Quantum chromodynamics (QCD) is non-perturbative at low energies where it is characterized by a scale separation. These two facts facilitate an approximate solution of low-energy QCD, *i.e.*, nuclear physics, with renormalization group (RG) and effective field theory (EFT) techniques [1–4].

The strongly interacting character of QCD is of particular interest at very low-energies. There, the nuclear regime can be described solely by nucleons interacting at the same space-time point, since the excitation of other degrees of freedom is dynamically forbidden. This “pionless” EFT (EFT($\not{\pi}$)) of nuclear physics is characterized by the large nucleon-nucleon (NN) scattering lengths relative to the effective range of the nuclear force, as indicated by the unnaturally small deuteron binding energy [5, 6]. EFT($\not{\pi}$) reproduces Bethe’s effective range theory [7] as an expansion of the NN amplitude about a non-trivial fixed point of the RG, *i.e.*, unitary fixed point. Thereby, it describes strongly interacting fermionic systems with infinite scattering lengths (original formulation [8, 9] and RG emphasis [10]) at its leading order (LO). For its usefulness in larger systems, EFT($\not{\pi}$) includes a 3-body contact interaction at LO, abandoning the naturalness assumption and naïve dimensional analysis for this operator. The enhancement of the 3-body-contact interaction is related to a limit cycle found in the RG analysis of the triton [11] and thereby also an expression of the specific regularization that facilitated the limit cycle and gave it its shape. The appearance of 3-body bound states at threshold associated with the limit cycle is a reminiscence of Efimov physics in the unitary limit [12]. Naïve power counting fails due to proximity to the non-trivial unitary fixed point. Perturbations at higher orders include effective-range corrections, as well as relativistic effects. Additional counter terms, needed to renormalize 3-nucleon forces in the triton, appear only at next-to-next-to leading order (NNLO) [13, 14].

The accidental separation of scales inducing the above EFT($\not{\pi}$) power counting is realized, in particular, between the large scattering lengths and the mass of the pion, as the lightest mesonic degree of freedom. The scale m_π suggests that the EFT($\not{\pi}$) approach is limited to light nuclei ($A \lesssim 4$), since the scale set by the binding momentum in heavier nuclei is of the order of the pion mass m_π , implying their mandatory explicit inclusion in the theory. As QCD generates this large scattering length, its effective potential between nuclei is, relative to the scattering length, short-ranged.

The existence of a long-range repulsive interaction, namely the Coulomb exchange between protons, complicates the description of nuclei relative to generic systems in the unitary limit which are canonically analyzed solely by means of short-range potentials.

The electromagnetic interaction plays an important role in many applications of nuclear physics. The importance of the Coulomb force, in particular, rises as the momentum scale decreases. This expectation follows from the naïve scale of the effect, $\frac{\alpha m_N}{Q}$, which becomes significant for momenta $Q \lesssim 10$ MeV (nucleon mass m_N , and fine structure constant α). Low-energy proton-proton scattering, *e.g.*, [15], is just one example representing a wealth of bound and scattering few-body systems where this enhancement requires an accurate description of the Coulomb force.

The conditions for a perturbative treatment for $A > 2$ are non-trivial to assess. The complexity is apparent in the seemingly contradictory observations of Coulomb effects only distorting the asymptotic wave function in the analysis of low-energy proton-proton scattering [16, 17], on the one hand, while on the other hand a new counter-term[18] is needed to fit the low-energy proton-proton scattering length [19]. The Helium-3 (helion) nucleus constitutes an ideal (and maybe the only, if EFT($\not{\pi}$) is inapplicable in heavier nuclei) nuclear specimen to study the effect of a long-range force on the dynamics of otherwise short-range interacting fermions.

The problem is of universal character as we understand nuclear physics as one representative of a class of theories which sit in the vicinity of a “critical manifold” in the space of 2 and 3-body coupling constants: an infrared fixed point and a limit cycle. In the presence of long-range forces, RG properties are changed significantly [20, 21]. Thus, nuclear physics at very low energies, characterized by the strong short-range forces of the unitary fixed point, and weak Coulomb long-range forces, provides a model, as well as a physical system.

EFT($\not{\pi}$) studies of Helium-3 with cutoff variation have been first accomplished in 2010 [22–24], validating the LO power counting. The recent helion analysis [25] is remarkable for its unnatural promotion of another 3-nucleon operator. From a cutoff dependence of the helion binding energy ($B(^3\text{He})$) at next-to-leading order (NLO), the enhancement of an isosymmetric 3-nucleon interaction to NLO was inferred. The nuclear bound state problem was formulated and solved, in that work, using Lippmann-Schwinger integral equations and the Coulomb interaction was included non-perturbatively. Here we use the analogous Schrödinger approach to solve the nuclear problem, which effectively imposes a cutoff on the

potential and in that differs from the method employed in [25]. In our scheme, results do not exhibit a strong cutoff dependence.

In this article, we present an EFT(π) calculation at NLO, including the renormalized Coulomb interaction. We outline a consistent scheme to study EFT(π) at NLO, and show that it is equivalent to the distorted-wave Born approximation. The predictive power is demonstrated in the Helium-3 system. Moreover, we show that the results are consistent with a perturbative treatment of the Coulomb force in this nucleus.

II. PERTURBATIVE NEXT-TO-LEADING ORDER EFT(π)

In this section, we summarize the power counting of the EFT(π) up to NLO. Power-counting schemes, in general, order contributions of the arbitrarily complicated interaction operators built of the nucleon field N and its derivatives, which appear in the effective Lagrangian, to the scattering amplitude. We elaborate on how this ordering is preserved in a calculation using solutions of the Schrödinger equation as the standard approach to systems beyond three bodies. To that end, the identity of a NLO-EFT(π) calculation and the familiar distorted-wave Born approximation (DWBA) is detailed.

A. EFT(π) for 2 and 3 nucleons

As shown in [26], the EFT(π) considers the most general Lagrangian built with nucleon fields and its derivatives. Initially, terms are ordered by their mass dimension and the tree-level amplitude is identified with a potential. In momentum space with incoming (outgoing) relative momentum \vec{p} (\vec{p}'), the latter is given by

$$V(\vec{p}, \vec{p}') = C_0 + C_2 (\vec{p}^2 + \vec{p}'^2) + \dots \quad . \quad (1)$$

2-body sector EFT(π) is an unnatural theory because in addition to the phenomena defining nuclear physics at the heavy mass scales m_N (nucleon mass) and M (breakdown scale $\sim m_\pi$), it has to incorporate a rich structure at the small scale $\aleph \sim B(D)$. The deuteron binding energy $B(D)$ is small relative to m_π , and the corresponding pole of the amplitude can be produced with an unnatural scaling of $C_0^{(R)} \sim 4\pi/(m_N \aleph)$. In comparison, in a natural theory, the renormalized (R) low-energy constant (LEC) $C_0^{(R)}$ associated with

a four-fermi operator is $C_0^{(R)} \sim 4\pi/(m_N M)$. Due to the unnatural scaling, all iterations (loops) of this interaction are of equal size and need to be considered at the same order of the EFT expansion.

It has been shown that $C_2^{(R)} \sim 4\pi/(m_N M \aleph^2)$, *i.e.*, the momentum-dependent interaction scales naturally in contrast to C_0 [27]. Each insertion of a C_2 vertex is suppressed by a factor of \aleph/M and contributes to the next higher order in the expansion of the amplitude.

The iteration of the momentum-independent LO interaction and the perturbative insertion of the NLO vertex is shown without reference to (iso) spin degrees of freedom in Fig. 5. We adopt this power-counting scheme for all NN channels.

In addition to the strong short-range force, electromagnetic interactions contribute significantly at low energies to the pp amplitude in form of static Coulomb-photon exchanges.

This exchange implies a different RG parameter dependence, and an iso-spin-dependent contact interaction has to be introduced to renormalize the pp channel [19].

3-body sector Until recently (see discussion of [25] below), 3-nucleon forces were thought to follow the same pattern in the spin-doublet channel. Namely, an unnatural enhancement of a momentum-independent 3-nucleon contact interaction due to the existence of a low-energy scale [13], and corrections from 3-nucleon terms in addition to the 2-nucleon operators which are included perturbatively at an order determined by dimensional analysis [14]. In this framework, the LO potential

$$V_{LO} = C_{0,s} \hat{P}^{(1S_0)} + C_{0,t} \hat{P}^{(3S_1)} + D \hat{P}^{(2S_{1/2})} \quad (2)$$

is iterated. It includes a LO 3-body interaction with LEC D in the $^2S_{1/2}$ channel. Predictions are then refined with a perturbative treatment of the NLO potential

$$V_{NLO} = \left(C_{2,s} \hat{P}^{(1S_0)} + C_{2,t} \hat{P}^{(3S_1)} \right) (\vec{p} - \vec{p}')^2 \quad (3)$$

which is projected ($\hat{P}^{(2S+1L_J)}$) into decoupled spin-singlet (s) and triplet (t) NN channels. As the interaction operates on antisymmetric states, it is sufficient to consider the squared momentum transfer of the in- and outgoing nucleon pair, $\vec{q} \equiv \vec{p} - \vec{p}'$. With that LO and NLO, EFT($\not{\pi}$) has been successful in describing the 3-nucleon system (LO [13] and NLO in [28]).

The Coulomb interaction The electromagnetic interaction between two protons is non-perturbative for relative momenta $Q \lesssim \alpha m_N \sim 10$ MeV. The momentum scale associated

with the bound-state pole in the helion channel, $k_{\text{typ}} = \sqrt{2m_N B(^3\text{He})/3} \sim 70$ MeV, is large enough for a perturbative treatment of the Coulomb interaction [29]. The perturbative approach would be inappropriate if states with relative pp momentum $Q < 10$ MeV contribute significantly to the helion bound state, as calculations (see [30] for a recent study) and measurements (*e.g.*, [31]) indicate [32].

In the following section, we explain how the power counting is implemented in a calculation of observables by solving the Schrödinger equation in coordinate representation.

B. Schrödinger formulation of EFT(π)

The NLO-EFT(π) amplitude expressed in terms of wave functions is given by

$$f_{l=0}(p) = -\frac{1}{p} \int_0^\infty dr \, r \, j_0(pr) (m_N V_{LO}) \psi_p^{LO}(r) - \frac{1}{p^2} \int_0^\infty dr \, (m_N V_{NLO}) (\psi_p^{LO}(r))^2 \quad (4)$$

which is known as the distorted-wave Born approximation for the two potentials $V_{LO} + V_{NLO}$ (the derivation and notation is given in Sec. A).

The potentials and associated amplitudes as recapitulated in the previous section need to be renormalized. In this context, the renormalization scheme comprises two steps (*a*), (*b*):

a. (*a*) *Regularization of the EFT(π) potential* We employ a cutoff scheme convenient for the numerical solution of Eq. A1 in coordinate space: The renormalized LECs (superscript Λ) in the 2-body potentials

$$V_{LO}^{\Lambda,2}(\vec{r}) = \left(C_{0,s}^\Lambda \hat{P}^{(^1S_0)} + C_{0,t}^\Lambda \hat{P}^{(^3S_1)} \right) e^{-\frac{\Lambda^2}{2} \vec{r}^2} \quad (5)$$

and

$$V_{NLO}^\Lambda(\vec{r}) = \left(C_{2,s}^\Lambda \hat{P}^{(^1S_0)} + C_{2,t}^\Lambda \hat{P}^{(^3S_1)} \right) \left[\frac{(\Lambda \vec{r})^2 - 6}{4} \right] e^{-\frac{\Lambda^2}{2} \vec{r}^2} \quad (6)$$

depend in contrast to the bare LECs in Eq. 2,3 on the regulator. A factor of $\Lambda^{3\{5\}}/(8\pi^{3/2})$ ($\{N\}LO$) from the Fourier transform of the momentum space regulator was lumped into the LECs.

Due to the non-perturbative character of the cutoff dependence of the 3-nucleon amplitude, the promoted 3-nucleon counter term has to be iterated as well [11, 13]. We regularize

this term such that its coordinate-space representation reads

$$V_{LO}^{\Lambda,3}(\vec{r}_1, \vec{r}_2) = \left(\frac{\Lambda^3}{8\pi^3/2} \right)^2 \cdot D^\Lambda e^{-\frac{\Lambda^2}{2}(\vec{r}_1^2 + \vec{r}_2^2)} \quad (7)$$

and adopt the power counting of [33] in which this is the only 3-body operator up to NLO in the triton channel. A LO-EFT($\not\Lambda$) calculation in the 3-body sector then proceeds by solving Eq. A1 with the sum of Eq. 5 and Eq. 7.

Based on the discussion above about typical momenta in the 3-nucleon bound system, we consider the Coulomb interaction as a perturbation *and* as a non-perturbative effect. As a perturbation, the Coulomb potential

$$V_C^\Lambda(\vec{r}) = C_{pp}^\Lambda \hat{P}_{pp}^{(1S_0)} e^{-\frac{\Lambda^2}{2}r^2} + \frac{e^2}{4|r|} \quad (8)$$

contributes in the same way as the NLO-EFT($\not\Lambda$) interaction in Eq. 6 to the 3-body amplitude (see cartoon in Fig. 1). Through the projector $\hat{P}_{pp}^{(1S_0)}$, the LEC C_{pp}^Λ acts between protons, only. The proper non-perturbative treatment defines a new LO potential as the sum of Eq. 5 and Eq. 8.

For the cutoff, we chose a range from 660 MeV to 2.4 GeV to cover an interval in which the results of [25] display significant cutoff dependence. As we employ a variational method to solve the 3-body problem, reaching convergence in excited states is numerically challenging. Thus we limit the analysis to this range where we can find one bound state below and two above a critical cutoff $\Lambda_{\text{crit.}} \sim 1230$ MeV.

b. (b) Calibration of LECs We calibrate/renormalize the LECs such that the amplitudes Eq. A4 (LO) and Eq. 4 (NLO) resemble appropriate data. Scattering phase shifts (δ) at low energy are the canonical choice. To express the corresponding amplitude in terms of effective-range parameters, two steps are involved: expand $p \cot \delta(p)$ about some p (effective-range expansion); expand the ensuing amplitude, $f(p) = (p \cot \delta - ip)^{-1}$, in a power series consistently, *i.e.*, about a momentum the EFT expansion is expected to converge rapidly, and up to the same power as the EFT.

At LO, we expand about $|\vec{p}| = 0$, and thus have to adjust the LECs such that the amplitude from Eq. A4 matches the scattering length (a) of the respective channel, $\lim_{p \rightarrow 0} f(p) = -a$. For the NLO calculation, it is prudent to expand about a momentum (p_0) which is typical for the system under investigation and *not* about zero[34]. The three-nucleon system contains the singlet and triplet states as subsystems and momentum scales in

those systems are given by the poles of the respective amplitude in the complex momentum plane:

$$\gamma = \pm i r^{-1} \left(1 - \sqrt{1 - 2ra^{-1}} \right) = \mp i_{45.7}^{7.88} \begin{smallmatrix} (S=0) \\ (S=1) \end{smallmatrix} \text{ MeV} . \quad (9)$$

The logical choice is thus: $p_0 = |\gamma|$ because we use positive energy scattering states as asymptotic boundary conditions to obtain amplitudes from Eq. A4,4). Explicitly, we match Eq. 4 to the *Taylor expansion* (we spare the reader the lengthy expression) of

$$f(p) = \left(-|\gamma| + \frac{r_0}{2}(\gamma^2 + p^2) - ip \right)^{-1} \quad (10)$$

about the pole $p_0 = |\gamma|$ in the NN singlet and triplet channel, respectively.

The LEC C_{pp}^Λ is renormalized to the pp scattering length, $a_{pp}^C = -7.81$ fm, by matching the pp amplitude to the generalized effective range expansion [35] for charged particles. For this calibration, the interaction in Eq. 8 is iterated because a_{pp}^C is extracted from the amplitude at momentum $\ll 1$ MeV. Whether or not the thus obtained C_{pp}^Λ does renormalize the 3-nucleon amplitudes, if considered perturbatively, as detailed below Eq. 8, validates or invalidates the power counting. We rely on a numerical calculation for this assessment. The renormalization scheme as defined above defies an analytic argument [36] because, first, the bare Coulomb wave functions are approximated and separately cut off at small distances, and second, because we do not regularize dimensionally but with a cutoff function.

c. Practical implementation of EFT(π) The LO LECs, $C_{0,s/pp}^\Lambda, C_{0,t}^\Lambda$, are calibrated by solving the Schrödinger equation A1 in coordinate representation and a matching of the corresponding amplitude Eq. A4 to the respective scattering length. For the 3-nucleon LEC, the thus obtained 2-body LECs are held fixed, while $D_{(*)}^\Lambda$ is adjusted such that Eq. A1 has a negative energy eigenvalue equal to $B(T)$ in the triton channel corresponding to the ground or first excited state (indicated by a $*$ and explained at the end of this section). We predict solely $B(^3\text{He})$ with this theory for a non-perturbative Coulomb interaction. If it is treated in perturbation theory, $B(^3\text{He}) = B(T)$ at LO.

At NLO, too, we first renormalize the 2-body sector. First, we minimize the difference between the DWBA amplitude Eq. 4 and the power expansion of Eq. 10. This minimization varies the LECs, $C_{0/2,s}^\Lambda, C_{0/2,t}^\Lambda$, from which the unperturbed wave functions are calculated as in LO above, until a termination condition is satisfied. The optimization starts with the LO values for $C_{0,s/t}^\Lambda$, and $C_{2,s/t}^\Lambda = 0$. The implied adjustment of LECs of momentum-independent vertices has an analog in the integral approach (see *e.g.*, [26]). For the calibration of $D_{(*)}^\Lambda$,

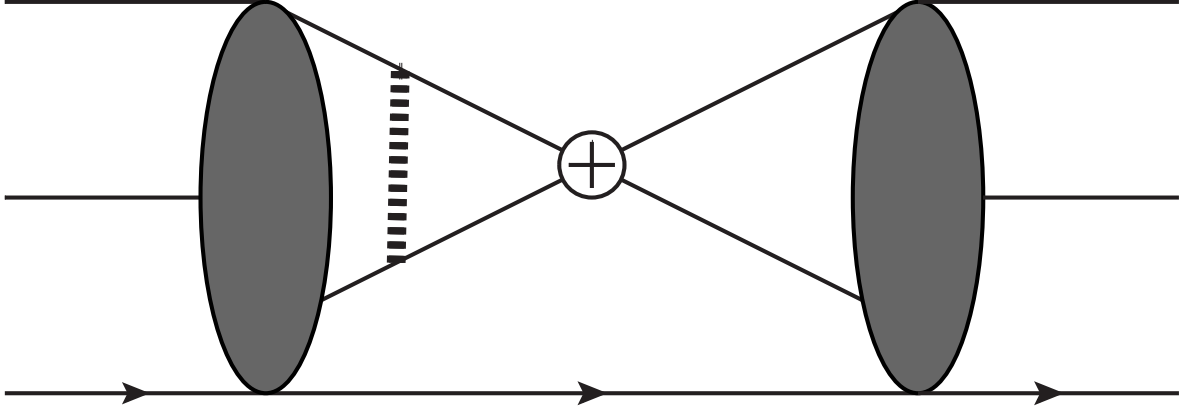


FIG. 1. Graphical representation of the lowest order Coulomb correction of the helion binding energy. Triton wave functions are indicated by gray-filled blobs with three incoming lines. An (no) arrow shows the forward time direction for neutrons (protons), the exchanged Coulomb photon dashed, and the pp vertex is the circle cross.

the 2-body LECs are fixed. With $C_{0,s/t}^\Lambda$, which *differ* from the LO values, and a trial $D_{(*)}^\Lambda$ a ground (excited) state wave function is calculated via Eq. A1. The energy eigenvalue of that state is shifted by the matrix element of that state and the NLO potential in Eq. 6. $D_{(*)}^\Lambda$ is optimized such that this sum equals the triton binding energy.

Thereby, renormalization constraints of NLO-EFT($\not\pi$) used in this work incorporate 6 data points: the neutron-proton scattering lengths and effective ranges for the singlet and triplet channel, the proton-proton scattering length, and the triton binding energy. The pp and np-singlet effective ranges were assumed to be identical, and hence the NLO interaction in Eq. 6 does not break iso-spin symmetry.

Noteworthy are the two renormalization conditions we employed for the 3-nucleon interaction. First, we identified the *shallowest* state of the nnp-spin-doublet system with the triton. This state can be the ground or an excited state, if the EFT tenet is adopted that effects of deep states, *i.e.*, composed predominantly of modes with momentum beyond the breakdown scale, on predictions of a renormalized EFT can be removed order by order. In a scenario where the 3-nucleon spectrum *without* 3-body force sustains two bound states (results in Fig. 2 (a) for $\Lambda > \Lambda_{\text{crit.}}$ or, *e.g.*, Fig. 6 in [13]), the adjustment of the 3-body parameter to fix the excited state to the triton will leave the deep state in the spectrum. The corresponding LEC D_*^Λ exhibits a discontinuous jump between two branches: a repulsive

branch (solid black in Fig. 2 (b)) which matches a deeply-bound ground state to the triton, and an attractive branch (dashed black Fig. 2 (b)) which lowers an excited state entering at $\sim \Lambda_{\text{crit.}}$ to the triton (see also the discussion of Figs. 4 and 3, below). The two branches do not resemble the log-periodic cutoff dependence of the dimensionless 3-body parameter found analytically with auxiliary dibaryon fields [11]. We assume that the running of our 3-body parameter continues periodically, too. While the detailed functional dependence of the cycle is regulator dependent, a constant ratio between the two shallowest 3-nucleon states is widely believed to be a universal feature of nuclei; all regulators must approximate the same ratio barring higher-order effects. The second assumption about the regulator employed here is thus: the second excited bound state which enters, considering the small slope of D_* at $\Lambda \gg 2.4$ GeV, has a binding energy which is relative to the first excited state in the same universal ratio as extrapolated from the calculated spectrum. From the red-dotted line in Fig. 2 (a), we find $B^{(1)}(3)/B^{(0)}(3)$ to converge to a value close to the universal ratio of $\sim 1/515$ which was derived for $a \rightarrow \pm\infty$ [12].

The *second* condition allows only one bound state in the spectrum and adjusts D^Λ to fix this state's energy to $B(\text{T})$. This LEC will not follow a limit cycle because even beyond the critical cutoff it adjusts the deep state and *not* the incoming shallow one. Hence, above some cutoff[37], this procedure will always produce a repulsive 3-body force (see thin gray line as continuation of solid black in Fig. 2 (b)).

d. Toolbox Optimization problems are solved with the *BFGS* quasi-Newton method [38] as implemented in the *numPy*-1.8.2 library. To obtain 2-body scattering wave functions, we alternated between three methods to minimize the possibility of a mistake in the numerical implementation of either method: a *Numerov* integration, a version [39] of the *variable phase* method, and a *variational* method with a Gaussian trial wave function. Three-body wave functions and matrix elements were calculated with the *refined-resonating-group method* ($\mathbb{R}\text{GM}$, original formulation: [40, 41]; refinement and triton/ ^3He implementation: [42, 43]) [44]. The variational $\mathbb{R}\text{GM}$, as applied here, is significantly less accurate than the Numerov integration and the variable-phase method. We estimated its dominant numerical uncertainty by a rescaling of the variational Gaussian width parameters. With fixed LECs, the variation in $B(^3\text{He})$, induced by this multiplication of the widths on the two Jacobi coordinates by factors $\in (0.2, 2)$, was found to be $\lesssim 0.1$ MeV.

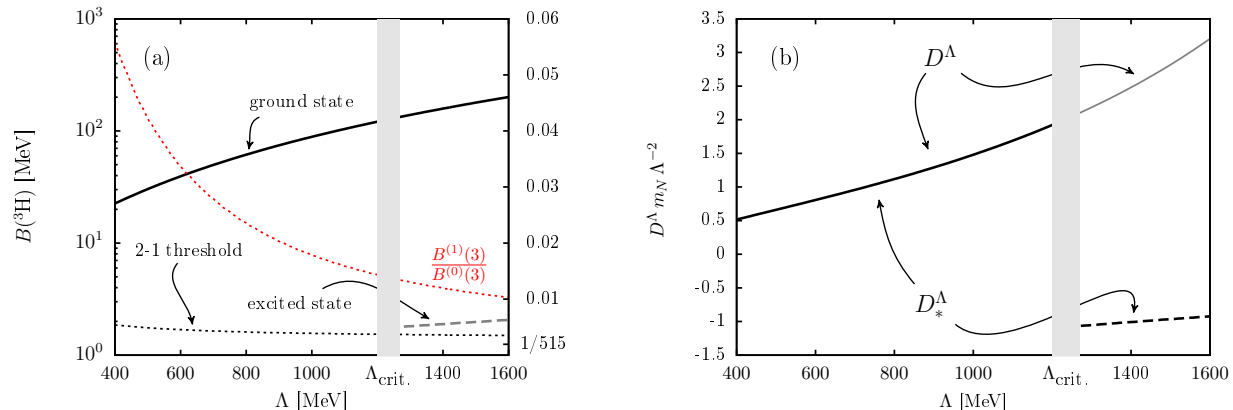


FIG. 2. Cutoff dependence of the ground (black solid) and first-excited-state (gray dashed) binding energies (left MeV Y-scale), and their ratio (dotted red, right Y scale) for $D_{(*)}^\Lambda = 0$ (panel (a)). In panel (b), the running of the dimensionless 3-nucleon LEC with the cutoff is shown. For $\Lambda \lesssim \Lambda_{\text{crit.}}$, only the ground state exists below the neutron-deuteron breakup threshold (thin dotted line (a)) with a corresponding repulsive 3-body LEC (solid black line (b)). For $\Lambda \gtrsim \Lambda_{\text{crit.}}$, an excited state appears, which can be matched to $B^{(1)}(3) \sim 8.5$ MeV with an attractive 3-body LEC (black dashed (b)), while the deeply-bound ground state requires an increasingly repulsive LEC (thin gray line (b)) to meet $B^{(0)}(3) \sim 8.5$ MeV.

III. HELIUM-3 RESULTS

The EFT($\not{\pi}$) as parameterized in the previous section was employed at LO and NLO to postdict the helion binding energy. Results are presented in Figs. 3 and 4 as functions of the cutoff to assess the sensitivity of the result to the renormalization scheme. This error analysis constitutes the canonical, *a posteriori* justification for the power counting of a cutoff EFT.

First, results with the *non-perturbative* Coulomb interaction are shown in Fig. 3. For both 3-body renormalization conditions, with (starry lines) and without the deep trimer, NLO results (solid lines) are found more stable for $\Lambda \rightarrow 2.4$ GeV than at LO (dashed) in the same limit. The total variation of $B(^3\text{He})$ over the considered cutoff range is highlighted in Figs. 3 and 4 by the height of overlapping rectangles. Comparing these uncertainties in $B(^3\text{He})$, we find the NLO results without a deep trimer about twice as accurate at NLO (blue, opaque rectangle at ~ 2.2 GeV) relative to LO (blue, transparent overlapping

rectangle). With a deep trimer, LO and NLO results are of about the same accuracy (red, overlapping opaque and transparent rectangles at ~ 2.3 GeV). The significant difference in LO uncertainties, depending on the chosen 3-body renormalization, with or without a deep state, exemplifies the need to test the renormalization-scheme independence beyond a cutoff-parameter variation with otherwise fixed regulator shape and identical matching conditions, *i.e.*, data input. A comprehensive analysis (see [45] for a recipe and [46] for its application), which would thus vary matching conditions and regulator shape, is required to assess the convergence rate of the EFT. Here, we aim to verify the consistency of the EFT's power counting, and it suffices to demonstrate convergence of predictions in a limit which removes the arbitrary regulator. To that end, we observe that the stability of all four curves for $\Lambda \rightarrow 2.4$ GeV does not indicate a failure of the power-counting of EFT($\not{\pi}$) up to NLO with a non-perturbative long-range Coulomb interaction.

If the Coulomb interaction is counted as a *perturbation*, the resultant postdiction for $B(^3\text{He})$ is shown in Fig. 4 (red line with circles). The LO result, in this counting scheme, coincides with the triton binding energy and is not shown as it is cutoff independent by construction. Treating the Coulomb interaction at the same order as the most significant momentum-dependent terms of EFT($\not{\pi}$) and *not* at LO, where the kinetic energy operator $\vec{\nabla}^2/(2m_N)$ and the 4- and 6-fermi momentum-independent terms are in balance to yield the shallow deuteron and triton states, is supported further by a comparison between the matrix elements (Eq. A7) of the Coulomb (Eq. 8) and NLO-EFT($\not{\pi}$) (Eq. 6) operators between LO triton wave functions. Both contributions, Coulomb and NLO to $B(^3\text{He})$ were found to be of $\mathcal{O}(1)$ in the considered cutoff interval while, in contrast, the kinetic energy and LO operators assume for $\Lambda > 1$ GeV values of $\mathcal{O}(10^2)$. In fact, perturbative Coulomb and NLO operators yield results close to the non-perturbative LO values (compare encircled solid and dashed lines in Fig. 4). This proximity is consistent with the key finding of this article, namely the perturbative character of the Coulomb interaction in ^3He . The iteration of the Coulomb exchange should then produce only higher-order-in- $\alpha m_N/Q$ corrections, which is precisely what we observe. Behavior like the increased splitting between the encircled solid perturbative NLO line and the dashed LO line in Fig. 4 for $\Lambda \gtrsim 2$ GeV is well within the limits of the numerical accuracy (± 0.1 MeV). Instabilities of that magnitude and shape (see also the step-like behavior of the star-dashed line in Fig. 3) are thus unlikely to resemble divergent components of the amplitude.

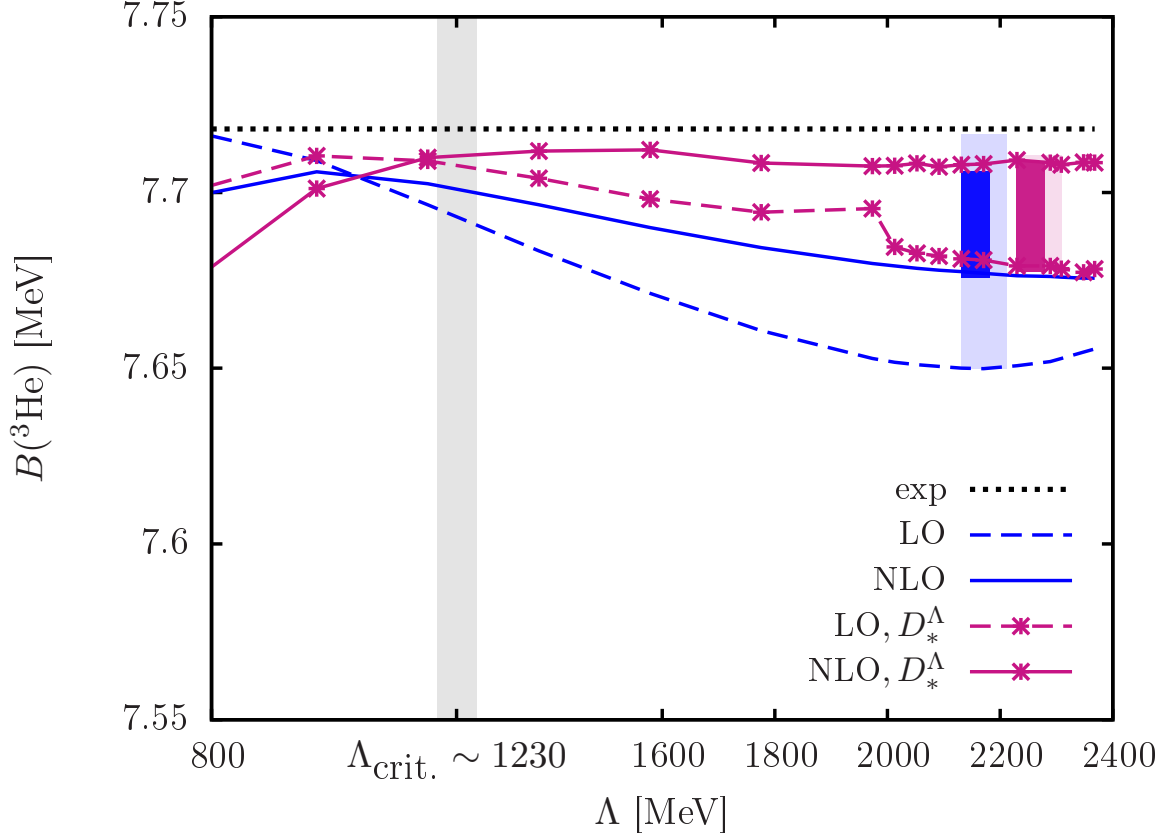


FIG. 3. The Helium-3 binding energy calculated from EFT($\not{\pi}$) with a *non-perturbative* Coulomb interaction. (NLO)LO results are shown as (solid)dashed lines and were obtained with the \mathbb{R} GM. Results admitting deep 3-body state in the spectrum, *i.e.*, Helium-3 is an excited state, are marked with stars. The assessed Λ uncertainty is indicated by the height of the transparent (LO) and opaque (NLO) rectangle. An additional 3-body bound state enters the spectrum (gray band) at $\Lambda_{\text{crit.}} \sim 1230$ MeV.

Assuming that the numerical uncertainty affects all results equally, shifting them by a similar amount if the variational parameters are refined, the dependence on Λ at NLO is found to be of the same magnitude as the LO uncertainty for non-perturbative Coulomb (compare transparent box height on the left with opaque height of the right box). Furthermore, the convergence with Λ is slower and has not yet reached a plateau at $\Lambda \sim 2.4$ GeV as in Fig. 3. The uncertainty represented by the height of the red opaque rectangle is thus nothing but a lower bound. The observed cutoff dependence is, however, not indicative for a failure of the power counting since the assessed lower bound of the uncertainty of ~ 0.1 MeV

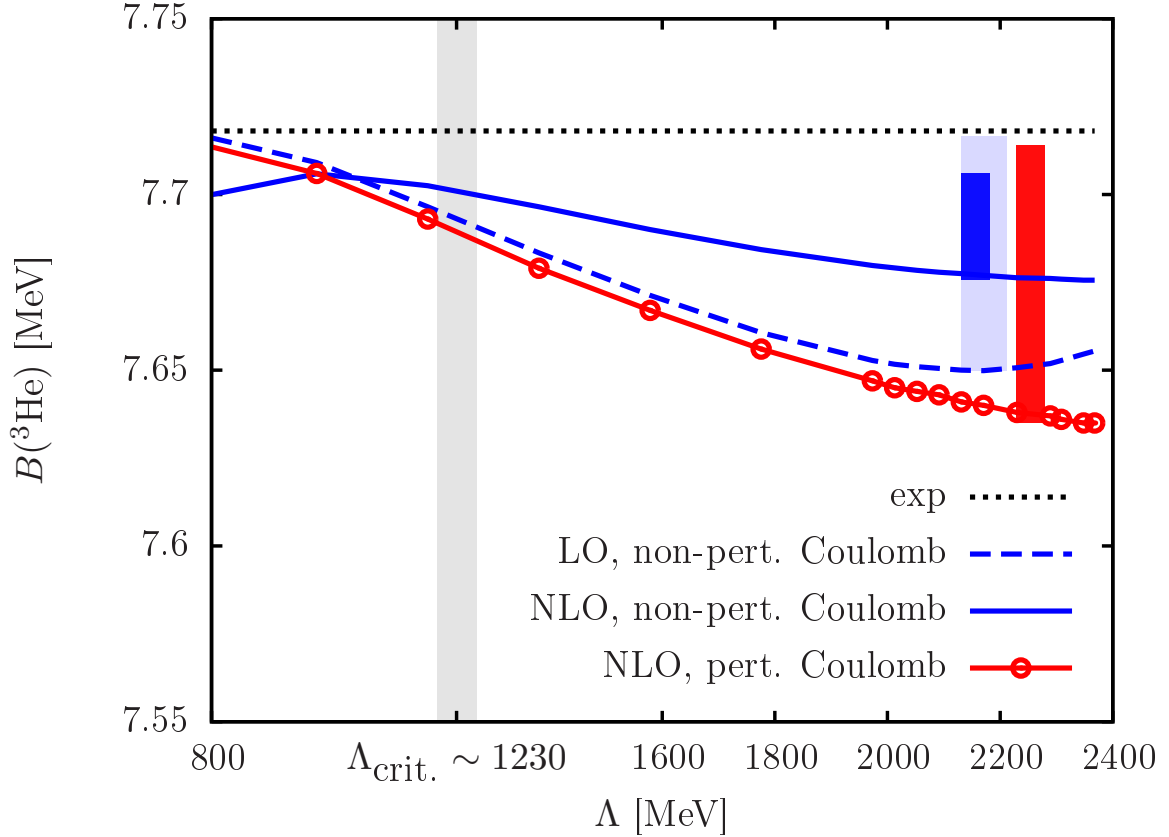


FIG. 4. Comparison between *perturbative* (circles) and *non-perturbative* (no marker) Coulomb treatment in Helium-3 with EFT(π). (NLO)LO results are shown as (solid)dashed lines. The horizontal dotted line represents the experimental ^3He binding energy. Transparent (LO) and opaque (NLO) rectangle heights indicate Λ uncertainty. At $\Lambda_{\text{crit.}} \sim 1230$ MeV (gray band), an additional 3-body bound state enters the spectrum.

is small compared with the 3-nucleon limit cycle [11] for $B(T)$, or the ~ 1.8 MeV change in $B(^3\text{He})$ found in the NLO analysis of Helium-3 [25] over the same cutoff range we cover.

Given the different regularization schemes and therefore RG trajectories followed by the respective Λ in [25] and this work, a comparison of the ranges in which Λ 's were varied is non-trivial. To assess whether or not sensitivity to short-distance structure is probed to the same extent with two arbitrary regularization schemes, comparing the ranges over which the respective parameters are varied is not productive. Here, we select an observable and compare cutoff ranges based on variations in that observable. Regulator variations are considered similar if they induce variations of the same order of magnitude in the observable.

For this observable, we chose the universal ratio of consecutive bound states in the 3-body system. We showed above (red-dotted line in Fig. 2 (a)) that our result for the binding-energy ratio of excited and ground state is almost converged and little variation is expected at higher cutoffs. Further cutoff variation will not increase the uncertainty in this observable and thus would not yield further insight to the renormalization-scheme dependence. In this metric, our cutoff range is comparable to the $\sim 10^5$ MeV-wide interval analyzed, *e.g.*, in [11].

In more detail, shallow 3-body states are created at threshold if no 3-nucleon force is adjusted and the two (in [25] the three) body regulator is varied. In the scheme employed here, the first of such states enters at a critical cutoff $\Lambda_{\text{crit.}} \sim 1230$ MeV (gray band in Figs. 3 and 4). In [25], the first divergence of the limit cycle of the LO 3-body LEC is located at a cutoff of ~ 1.8 GeV. The next bound state enters the spectrum at ~ 36 GeV in [25]. For our method it is impractical to probe Λ values that high. Nevertheless, assuming our cutoff scheme would require a similar counter term as the one promoted in [25], the cutoff range between 0.6 MeV and 2.4 GeV assessed here should suffice. In this range, the NLO 3-body LEC of [25] completes almost a complete cycle including zero. As the frequencies of the LO and NLO limit cycles (compare Figs. 6 and 9 in [25]) are similar and the first LO divergence occurs almost at the same cutoff value, we naïvely expect a similar $B(^3\text{He})$ variation as in [25]. However, the change we observe in the helion binding energy within this cutoff range is an order of magnitude smaller — note the y-scale in Figs. 3 and 4 spans only 200 keV — and thereby consistent within the EFT and numerical uncertainty.

To conclude, a power counting with LO comprised by the kinetic, three 4-fermi (pp , np singlet/triplet) and one 6-fermi operator treated non-perturbatively, and NLO adding perturbatively two momentum-dependent 4-fermi interactions is valid for the description of the 2 and 3-nucleon bound states. This counting is useful regardless of including the Coulomb interaction perturbatively or non-perturbatively. We argued that the seeming difference to the work of [25], in the case of a non-perturbative Coulomb force, is related to the regularization scheme which has a significant impact on the power counting.

IV. CONCLUSION

The renormalization-group dependence of the helion ground state was analyzed with the $\text{EFT}(\pi)$. The binding energy of that state was found invariant with respect to an RG parameter which rescales the 2- and 3-body interaction in a similar fashion. The residual uncertainty in this next-to-leading-order analysis was found insensitive to the iteration of the exchange of Coulomb photons, thus justifying their perturbative treatment.

The result seemingly contrasts an analysis with a non-perturbative Coulomb interaction formulating the few-body problem with auxiliary fields as a set of Lippmann-Schwinger equations. As both formulations are identical except for the regularization and the RG flow thereby parameterized, we stress that despite the suggestive Λ nomenclature common to both calculations, the methods differ significantly in that procedure. The dimensional regulator for the 2-body combined with the cutoff regulator in the 3-body propagator follow a critical trajectory while the regularization chosen in this work does not. This difference between combining dimensional regularization with power divergence subtraction (PDS) with a cutoff regulator [25], on the one hand, to a cutoff-regulated theory for both the 2- and 3-nucleon amplitudes on the other hand is an unsolved problem. Its importance reaches beyond $\text{EFT}(\pi)$, considering the analytical and numerical efforts to match chiral effective theories with $\text{EFT}(\pi)$ to determine the quark-mass dependence of the nuclear force rigorously ([47] and [28] are EFT-inspired models in that direction): chiral interactions for few-body systems are completely cutoff regulated while $\text{EFT}(\pi)$, barring [29, 48, 49], implementations mix cutoff with dimensional-PDS regularization. The discrepancy uncovered here, shows that the two schemes differ in the presence of a long-range interaction, namely the Coulomb force, and thus asks for a generalization of the analysis of [10] to the three-body sector.

The above methodology of solving $\text{EFT}(\pi)$ in coordinate space with a regulated 2- and 3-body potential was chosen for its practicality to analyze larger nuclei. Regardless of the applicability of $\text{EFT}(\pi)$ in the 4-nucleon system and beyond, the larger momentum scale in those nuclei suggests that a perturbative treatment of the Coulomb interaction for their ground states converges even faster than in helion. Even for Helium-3 and the triton, our results do not rely on $\text{EFT}(\pi)$ as the short-distance interaction. A perturbative Coulomb force will be useful for any nuclear interaction describing consistently the 2-nucleon scattering lengths and effective ranges, and the triton ground state.

Considering the ongoing struggle in finding a RG invariant formulation of chiral perturbation theory for few-nucleon systems [50–54], we conclude with noting the intriguing application of the above treatment of photons, *i.e.*, iterated and renormalized in the 2-body sector and as a perturbation in larger systems, to pions[55].

Appendix A: The distorted-wave-Born amplitude

We recapitulate the distorted-wave Born approximation of a scattering amplitude for the sum of two potentials: the short-range strong interaction, for which the Schrödinger equation is solved, and the long-range Coulomb interaction augmented with short-range operators, which are then considered as a perturbation. We follow the standard of Taylor [56].

The full scattering states $|\vec{p}\pm\rangle_V$ corresponding to an interaction V and in/outgoing boundary conditions (\pm) obey the stationary Schrödinger *differential* equation

$$(H_0 + V) |\vec{p}\pm\rangle_V = E_p |\vec{p}\pm\rangle_V . \quad (\text{A1})$$

The wave function $\psi_p^V(\vec{r}) = \langle \vec{r} | \vec{p}\pm \rangle_V$ with $E_p = p^2/m_N$ can also be obtained from the Lippmann-Schwinger *integral* equation

$$\langle \vec{r} | \vec{p}\pm \rangle_V = \langle \vec{r} | \vec{p} \rangle_0 + \langle \vec{r} | G_0(E_p \pm i\epsilon) V | \vec{p}\pm \rangle_V . \quad (\text{A2})$$

A free state $|\vec{p}\rangle_0$ and the Green's operator G_0 follow from Eq. A1 with $V = 0$. The T operator acts in the space of free states and is introduced as $T(E_p \pm i\epsilon) |\vec{p}\rangle_0 = V |\vec{p}\pm\rangle_V$. In terms of T , Eq. A2 reads

$$\begin{aligned} {}_0\langle \vec{p}' | T | \vec{p} \rangle_0 &= {}_0\langle \vec{p}' | V | \vec{p} \rangle_0 + {}_0\langle \vec{p}' | V G_0 T | \vec{p} \rangle_0 \\ &= {}_0\langle \vec{p}' | V | \vec{p} \rangle_0 + {}_0\langle \vec{p}' | V G_0 V + V G_0 V G_0 V | \vec{p} \rangle_0 \\ &\quad + \dots , \end{aligned} \quad (\text{A3})$$

where the iterative solution in the second line is graphically represented by the diagrams in the first line of Fig. 5 if $V = V_{LO}$. The full amplitude calculated via

$$\begin{aligned} f_l(p) &= -m_N \int_0^\infty dr r^2 {}_0\langle \vec{p}' | \vec{r} \rangle V \langle \vec{r} | \vec{p}\pm \rangle_{LO} \\ &\stackrel{l=0}{=} -\frac{1}{p} \int_0^\infty dr r j_0(pr) (m_N V) \psi_p^{LO}(r) \end{aligned} \quad (\text{A4})$$

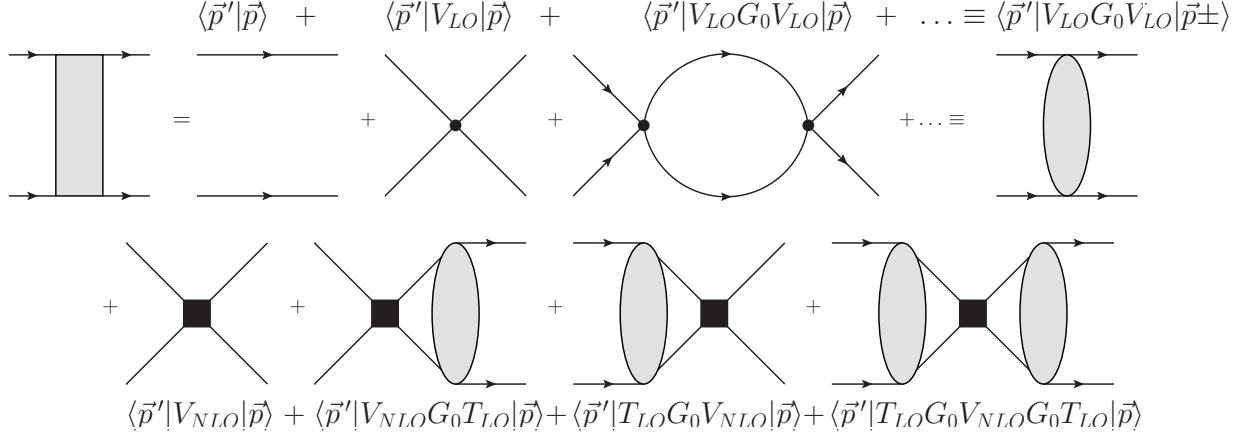


FIG. 5. Diagrammatic representation of the NLO-EFT(π) amplitude (gray, filled rectangle) as given in Eq. 4. The LO amplitude (gray, filled blob) is defined in the first line with free in and outgoing states with relative momenta \vec{p} and \vec{p}' . The perturbative insertion of the NLO vertex (square, Eq.3) is shown in the second line.

is thus identical to the one obtained from

$$f_{l=0}(p) = {}_0\langle \vec{p}' | T(E_p \pm i\epsilon) | \vec{p} \rangle_0 \quad . \quad (\text{A5})$$

In the EFT(π) power counting, a coupling to partial waves with $l > 0$ becomes relevant beyond NLO. With $p \equiv (m_N E_p)^{1/2}$, spherical Bessel function, j_0 , and the radial wave function solving $(\partial_r^2 - m_N V + p^2)\psi_p(r) = 0$ we follow the notation of [56]. The LO-EFT(π) amplitude is thus either calculated via Eq. A4 with a wave function which is the solution of a differential equation, or as the solution of an integral equation (Eq. A3 and Fig. 5 first line). However, to solve Eq. A3, knowledge of the free wave functions $\langle \vec{r} | \vec{p} \rangle_0$ is needed.

Reformulating Eq. A4 in a basis given by the full LO solutions, $\langle \vec{r} | \vec{p} \pm \rangle_{LO}$, the Born approximation yields the NLO-EFT(π) amplitude as shown in Fig. 5. To see this, one identifies $H_0 \equiv T_{\text{kin}} + V_{LO}$ and $V \equiv V_{NLO}$. Now, assuming $|\vec{p} \pm \rangle_{LO} = |\vec{p} \rangle_0 + G_0(E_p \pm i\epsilon)V_{LO}|\vec{p} \pm \rangle_{LO}$ can be solved, Eq. A3 for the full (*not yet* NLO) amplitude is

$${}_0\langle \vec{p}' | T | \vec{p} \rangle_0 = {}_{LO}\langle \vec{p}' | V_{LO} | \vec{p} \rangle_0 + {}_{LO}\langle \vec{p}' | V_{NLO} | \vec{p} \pm \rangle_{NLO} \quad . \quad (\text{A6})$$

Approximating the full solution

$$|\vec{p} \pm \rangle_{NLO} \approx |\vec{p} \pm \rangle_{LO} = |\vec{p} \rangle_0 + G_0 T_{LO} |\vec{p} \rangle_0$$

yields for the second term in Eq. A6:

$$\begin{aligned}
{}_{LO}\langle \vec{p}' | V_{NLO} | \vec{p} + \rangle_{NLO} &\approx {}_0\langle \vec{p}' | V_{NLO} | \vec{p} \rangle_0 + {}_0\langle \vec{p}' | T_{LO} G_0 V_{NLO} | \vec{p} \rangle_0 \\
&\quad + {}_0\langle \vec{p}' | V_{NLO} G_0 T_{LO} | \vec{p} \rangle_0 + {}_0\langle \vec{p}' | T_{LO} G_0 V_{NLO} G_0 T_{LO} | \vec{p} \rangle_0 \\
&= {}_{LO}\langle \vec{p}' | V_{NLO} | \vec{p} + \rangle_{LO}
\end{aligned} \tag{A7}$$

with each term represented by a diagram in the second line in Fig. 5. Substituted in Eq. A6 yields Eq. 4.

ACKNOWLEDGMENTS

JK gratefully acknowledges the hospitality of the Ohio State University, discussions with N. Barnea, H. Deleon, R. J. Furnstahl, U. van Kolck, S. König, J. Vanasse, and the financial support of the Minerva Foundation. DG was supported, in part, by BMBF ARCHES. Both authors are grateful for U. van Kolck's and B. Bazak's comments on the manuscript.

-
- [1] S. Weinberg. Phenomenological Lagrangians. *Physica A Statistical Mechanics and its Applications*, 96:327–340, April 1979.
 - [2] S. Weinberg. Nuclear forces from chiral lagrangians. *Physics Letters B*, 251:288–292, November 1990.
 - [3] S. Weinberg. Effective chiral lagrangians for nucleon-pion interactions and nuclear forces. *Nuclear Physics B*, 363:3–18, September 1991.
 - [4] J. Gasser and H. Leutwyler. Chiral perturbation theory to one loop. *Annals of Physics*, 158:142–210, November 1984.
 - [5] H. Bethe and R. Peierls. Quantum theory of the dipion. *Proceedings of the Royal Society of London A: Mathematical, Physical and Engineering Sciences*, 148(863):146–156, 1935.
 - [6] H. A. Bethe and R. Peierls. The scattering of neutrons by protons. *Proceedings of the Royal Society of London A: Mathematical, Physical and Engineering Sciences*, 149(866):176–183, 1935.
 - [7] H. A. Bethe. Theory of the effective range in nuclear scattering. *Phys. Rev.*, 76:38–50, Jul 1949.

- [8] U. van Kolck. Effective field theory of short-range forces. *Nuclear Physics A*, 645(2):273 – 302, 1999.
- [9] D. B. Kaplan, M. J. Savage, and M. B. Wise. A New expansion for nucleon-nucleon interactions. *Phys. Lett.*, B424:390–396, 1998.
- [10] M. C. Birse, J. A. McGovern, and Keith G Richardson. A renormalisation-group treatment of two-body scattering. *Physics Letters B*, 464(34):169 – 176, 1999.
- [11] P. F. Bedaque, H.-W. Hammer, and U. van Kolck. Renormalization of the three-body system with short-range interactions. *Phys. Rev. Lett.*, 82:463–467, Jan 1999.
- [12] V. Efimov. Energy levels arising from resonant two-body forces in a three-body system. *Physics Letters B*, 33:563–564, December 1970.
- [13] P. F. Bedaque, H. W. Hammer, and U. van Kolck. Effective theory of the triton. *Nucl. Phys.*, A676:357–370, 2000.
- [14] H. W. Griesshammer. Naive dimensional analysis for three-body forces without pions. *Nucl. Phys.*, A760:110–138, 2005.
- [15] X. Kong and F. Ravndal. Proton proton fusion in leading order of effective field theory. *Nucl. Phys.*, A656:421–429, 1999.
- [16] G. F. Chew and M. L. Goldberger. On the analysis of nucleon-nucleon scattering experiments. *Phys. Rev.*, 75:1637–1644, Jun 1949.
- [17] J. D. Jackson and J. M. Blatt. The interpretation of low energy proton-proton scattering. *Rev. Mod. Phys.*, 22:77–118, Jan 1950.
- [18] This term is small relative to its analog in the neutron-proton channels which reconciles the two statements, eventually.
- [19] X. Kong and F. Ravndal. Coulomb effects in low energy proton-proton scattering. *Nuclear Physics A*, 665(1-2):137 – 163, 2000.
- [20] M. E. Fisher, S.-k. Ma, and B. G. Nickel. Critical exponents for long-range interactions. *Phys. Rev. Lett.*, 29:917–920, Oct 1972.
- [21] T. Barford and M. C. Birse. Renormalization group approach to two-body scattering in the presence of long-range forces. *Phys. Rev. C*, 67:064006, Jun 2003.
- [22] S.-i. Ando and M. C. Birse. Effective field theory of ^3He . *Journal of Physics G Nuclear Physics*, 37(10):105108, October 2010.

- [23] S. König and H.-W. Hammer. Low-energy p - d scattering and ${}^3\text{He}$ in pionless effective field theory. *Phys. Rev. C*, 83:064001, Jun 2011.
- [24] S. König and H.-W. Hammer. The low-energy p - d system in pionless eft. *Few-Body Systems*, 54(1-4):231–234, 2013.
- [25] J. Vanasse, D. A. Egolf, J. Kerin, S. König, and R. P. Springer. ${}^3\text{He}$ and pd scattering to next-to-leading order in pionless effective field theory. *Phys. Rev. C*, 89:064003, Jun 2014.
- [26] U. van Kolck. Effective field theory of short range forces. *Nucl. Phys.*, A645:273–302, 1999.
- [27] See [57] for a visualization of the different scalings.
- [28] H. W. Hammer, D. R. Phillips, and L. Platter. Pion-mass dependence of three-nucleon observables. *Eur. Phys. J.*, A32:335–347, 2007.
- [29] I. Stetcu, B. R. Barrett, and U. van Kolck. No-core shell model in an effective-field-theory framework. *Phys. Lett.*, B653:358–362, 2007.
- [30] R. B. Wiringa, R. Schiavilla, Steven C. Pieper, and J. Carlson. Nucleon and nucleon-pair momentum distributions in $A \leq 12$ nuclei. *Phys. Rev.*, C89(2):024305, 2014.
- [31] E. Jans, P. Barreau, M. Bernheim, J. M. Finn, J. Morgenstern, J. Mougey, D. Tarnowski, S. Turck-Chieze, S. Frullani, F. Garibaldi, G. P. Capitani, E. de Sanctis, M. K. Brussel, and I. Sick. Quasifree $(e, e'p)$ reaction on ${}^3\text{He}$. *Phys. Rev. Lett.*, 49:974–978, Oct 1982.
- [32] [30, 31] extract occupation numbers. However, it was shown [58] that occupation numbers cannot be defined uniquely. We therefore interpret the large contribution of low-momentum modes of [30, 31] as specific to the employed interaction and extraction method.
- [33] P. F. Bedaque, G. Rupak, H. W. Griesshammer, and H.-W. Hammer. Low-energy expansion in the three-body system to all orders and the triton channel. *Nucl. Phys.*, A714:589–610, 2003.
- [34] See Bethe’s original ERE expansion about the deuteron pole [7] or the fixing of the residue in [59] as examples of wise choices for the momenta to expand about.
- [35] L. P. Kok, J. W. de Maag, H. H. Brouwer, and H. van Haeringen. Formulas for the δ -shell-plus-coulomb potential for all partial waves. *Phys. Rev. C*, 26:2381–2396, Dec 1982.
- [36] As one presumably given in [60], where the authors address the same complex as this article does, and of which we became aware while finalizing this manuscript.
- [37] Here, this value is apparently < 400 MeV.

- [38] J. Nocedal and S.J. Wright. *Numerical Optimization*. Springer Series in Operations Research. Springer, 1999.
- [39] H. Ouerdane, M. J. Jamieson, D. Vrinceanu, and M. J. Cavagnero. The variable phase method used to calculate and correct scattering lengths. *Journal of Physics B: Atomic, Molecular and Optical Physics*, 36(19):4055, 2003.
- [40] J. A. Wheeler. Molecular Viewpoints in Nuclear Structure. *Phys. Rev.*, 52:1083–1106, 1937.
- [41] J. A. Wheeler. On the Mathematical Description of Light Nuclei by the Method of Resonating Group Structure. *Phys. Rev.*, 52:1107–1122, 1937.
- [42] H.M. Hofmann. In L.S. Ferreira, A.C. Fonseca, and L. Streit, editors, *Proceedings of Models and Methods in Few-Body Physics, Lisboa, Portugal*, page 243, 1986.
- [43] J. Kirscher and D. R. Phillips. Constraining the neutron-neutron scattering length using the effective field theory without explicit pions. *Phys. Rev.*, C84:054004, 2011.
- [44] As the \mathbb{R} GGM is readily replaced with another method, all necessary techniques are standard and the described implementation can easily be reproduced.
- [45] R. J. Furnstahl, D. R. Phillips, and S. Wesolowski. A recipe for EFT uncertainty quantification in nuclear physics. *J. Phys.*, G42(3):034028, 2015.
- [46] E. Epelbaum, H. Krebs, and U. G. Meißner. Precision nucleon-nucleon potential at fifth order in the chiral expansion. *Phys. Rev. Lett.*, 115(12):122301, 2015.
- [47] E. Epelbaum, U.-G. Meißner, and W. Glöckle. Nuclear forces in the chiral limit. *Nucl. Phys.*, A714:535–574, 2003.
- [48] J. Kirscher, H. W. Griedhammer, D. Shukla, and H. M. Hofmann. Universal Correlations in Pion-less EFT with the Resonating Group Model: Three and Four Nucleons. *Eur. Phys. J.*, A44:239–256, 2010.
- [49] L. Platter, H. W. Hammer, and Ulf-G. Meißner. On the correlation between the binding energies of the triton and the alpha-particle. *Phys. Lett.*, B607:254–258, 2005.
- [50] A. Nogga, R. G. E. Timmermans, and U. van Kolck. Renormalization of one-pion exchange and power counting. *Phys. Rev.*, C72:054006, 2005.
- [51] B. Long and C. J. Yang. Renormalizing Chiral Nuclear Forces: Triplet Channels. *Phys. Rev.*, C85:034002, 2012.
- [52] B. Long and C. J. Yang. Short-range nuclear forces in singlet channels. *Phys. Rev.*, C86:024001, 2012.

- [53] M. P. Valderrama. Perturbative Renormalizability of Chiral Two Pion Exchange in Nucleon-Nucleon Scattering: P- and D-waves. *Phys. Rev.*, C84:064002, 2011.
- [54] M. P. Valderrama. Perturbative renormalizability of chiral two pion exchange in nucleon-nucleon scattering. *Phys. Rev.*, C83:024003, 2011.
- [55] [61] is a recent example for reinterpreting a methodology originally devised for long-range Coulomb and short-range nuclear interactions through an identification of the pion-exchange as long ranged.
- [56] J. R. Taylor. *Scattering Theory*. Wiley, 1972.
- [57] J. Rotureau, I. Stetcu, B. R. Barrett, and U. van Kolck. Two and Three Nucleons in a Trap and the Continuum Limit. *Phys. Rev.*, C85:034003, 2012.
- [58] R. J. Furnstahl and H. W. Hammer. Are occupation numbers observable? *Phys. Lett.*, B531:203–208, 2002.
- [59] D. R. Phillips, G. Rupak, and M. J. Savage. Improving the convergence of N N effective field theory. *Phys. Lett.*, B473:209–218, 2000.
- [60] S. König, H. W. Griedhammer, H. W. Hammer, and U. van Kolck. Effective Theory of ^3H and ^3He . 2015.
- [61] V. Baru, E. Epelbaum, A. A. Filin, and J. Gegelia. Low-energy theorems for nucleon-nucleon scattering at unphysical pion masses. *Phys. Rev.*, C92(1):014001, 2015.